



KIT Is Required for Fetal Liver Hematopoiesis

Alessandro Fantin^{1,2*}, Carlotta Tacconi², Emanuela Villa², Elena Ceccacci³, Laura Denti¹ and Christiana Ruhrberg^{1*}

¹ UCL Institute of Ophthalmology, University College London, London, United Kingdom, ² Department of Biosciences, University of Milan, Milan, Italy, ³ Department of Experimental Oncology, IEO, European Institute of Oncology IRCCS, Milan, Italy

OPEN ACCESS

Edited by:

Emanuele Azzoni,
University of Milano Bicocca, Italy

Reviewed by:

Valerie Kouskoff,
The University of Manchester,
United Kingdom
Samanta Mariani,
University of Edinburgh,
United Kingdom

*Correspondence:

Alessandro Fantin
alessandro.fantin@unimi.it
Christiana Ruhrberg
c.ruhrberg@ucl.ac.uk

Specialty section:

This article was submitted to
Stem Cell Research,
a section of the journal
Frontiers in Cell and Developmental
Biology

Received: 01 January 2021

Accepted: 23 June 2021

Published: 29 July 2021

Citation:

Fantin A, Tacconi C, Villa E,
Ceccacci E, Denti L and Ruhrberg C
(2021) KIT Is Required for Fetal Liver
Hematopoiesis.
Front. Cell Dev. Biol. 9:648630.
doi: 10.3389/fcell.2021.648630

In the mouse embryo, endothelial cell (EC) progenitors almost concomitantly give rise to the first blood vessels in the yolk sac and the large vessels of the embryo proper. Although the first blood cells form in the yolk sac before blood vessels have assembled, consecutive waves of hematopoietic progenitors subsequently bud from hemogenic endothelium located within the wall of yolk sac and large intraembryonic vessels in a process termed endothelial-to-hematopoietic transition (endoHT). The receptor tyrosine kinase KIT is required for late embryonic erythropoiesis, but KIT is also expressed in hematopoietic progenitors that arise via endoHT from yolk sac hemogenic endothelium to generate early, transient hematopoietic waves. However, it remains unclear whether KIT has essential roles in early hematopoiesis. Here, we have combined single-cell expression studies with the analysis of knockout mice to show that KIT is dispensable for yolk sac endoHT but required for transient definitive hematopoiesis in the fetal liver.

Keywords: KIT, hemogenic endothelium, erythromyeloid progenitors, yolk sac, fetal liver

INTRODUCTION

Several consecutive waves of hematopoietic progenitors arise and contribute blood and immune cells to the growing vertebrate embryo in close spatiotemporal proximity to developing blood vessels (Hoeffel and Ginhoux, 2018). The first primitive hematopoietic precursors originate in the yolk sac blood islands between E7.0 and E8.25 in the mouse and differentiate into embryonic erythrocytes and yolk sac macrophages (Ginhoux and Guillems, 2016; Hoeffel and Ginhoux, 2018; Canu and Ruhrberg, 2021). These yolk sac macrophages colonize the embryo and differentiate into tissue-resident macrophages. The transient definitive wave of hematopoietic precursors arises when a subset of ECs in the yolk sac specializes into hemogenic endothelium to undergo an endothelial-to-hematopoietic transition (endoHT) between E8.5 and E9.5 in the mouse (Hoeffel and Ginhoux, 2018). This process generates erythromyeloid progenitors (EMPs), which leave the yolk sac after the onset of blood flow and colonize the liver (Lux et al., 2008; Frame et al., 2013; McGrath et al., 2015; Hoeffel et al., 2015; Hoeffel and Ginhoux, 2018). In the liver, EMPs give rise to both transient definitive erythrocytes and monocyte precursors for tissue macrophages. It is thought that the liver EMP-derived macrophages replace the initial pool of yolk sac-derived macrophages in all organs, with the exception of the tissue-resident macrophages of the central nervous system, termed microglia (Hashimoto et al., 2013; Hoeffel et al., 2015). Finally, the definitive wave of hematopoietic precursors emerges via endoHT in the aorta-gonad-mesonephros (AGM) region

(Sanchez et al., 1996; Yokomizo and Dzierzak, 2010) as a continuum of pro-, pre-, and definitive hematopoietic stem cells (HSCs) that seed the liver from E10.5 in the mouse before colonizing the bone marrow just before birth (Taoudi et al., 2008; Rybtsov et al., 2014, 2011; Azzoni et al., 2018).

Hemogenic ECs are induced by retinoic acid signaling, which upregulates the expression of the receptor tyrosine kinase KIT (Dejana et al., 2017), whereby KIT cell surface expression is often used as a distinguishing feature from non-blood-forming ECs (Goldie et al., 2008). Moreover, KIT is also used as a key marker for the progeny of hemogenic endothelium, including EMPs (Gomez Perdiguero et al., 2015; Hoeffel et al., 2015; McGrath et al., 2015) and HSCs (Sanchez et al., 1996; Gomez Perdiguero et al., 2015). Genetic defects that disrupt KIT signaling reduce the number of late embryonic HSCs (Ikuta and Weissman, 1992), affect lymphopoiesis in the adult (Waskow et al., 2002), and cause severe macrocytic anemia and thus late embryonic or perinatal lethality (Bernex et al., 1996; Broudy, 1997; Ding et al., 2012). The anemic phenotype was ascribed to an erythroid differentiation block in the fetal liver after E13.5 (Chui and Russell, 1974; Chui and Loyer, 1975; Chui et al., 1978; Broudy, 1997) that could be rescued by wild-type HSCs (Fleischman and Mintz, 1979) or by erythropoietin overexpression (Waskow et al., 2004). Subsequent studies with function-blocking antibodies further suggested that hematopoietic waves originating before E12.5 depend less on KIT than later embryonic waves (Ogawa et al., 1993). However, it has not been directly addressed whether KIT is required for yolk sac endoHT, EMP formation, or EMP function.

Here, we have combined confocal imaging, single-cell transcriptomic analyses, and flow cytometry to identify the cellular profile of *Kit* expression during early hematopoiesis in the mouse. Our functional studies further show that the hematopoietic requirement for KIT does not comprise yolk sac hematopoiesis, including the generation of EMPs. Instead, we find that KIT is required for EMP expansion and the EMP-dependent process of transient-definitive hematopoiesis that takes place in the fetal liver and includes the generation of fetal erythroid cells. KIT is therefore required for erythropoiesis earlier than previously reported. These conclusions agree with those in prior studies of mice lacking the KIT ligand KITL, also known as stem cell factor (SCF) (Azzoni et al., 2018).

RESULTS

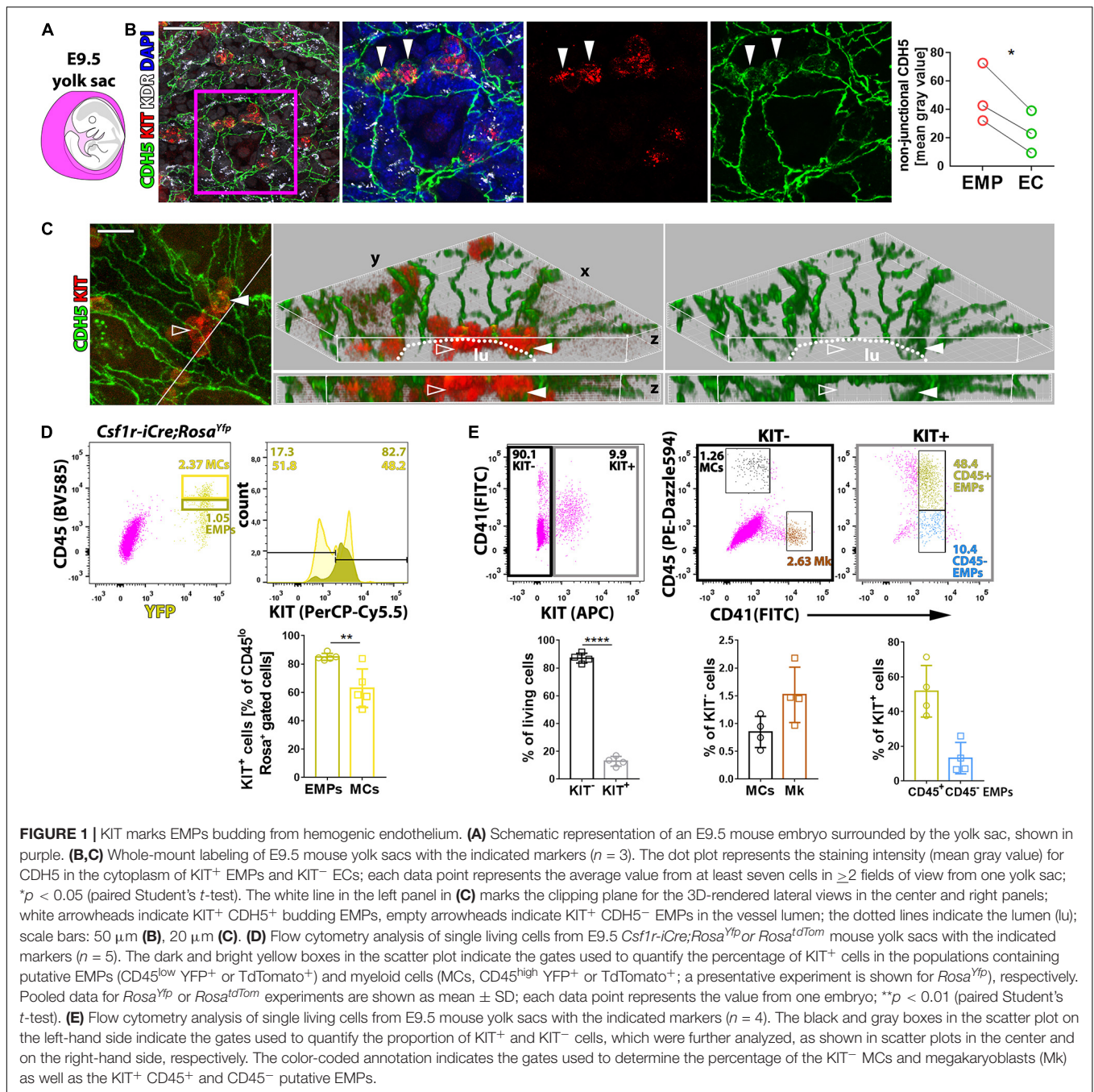
KIT Marks EMPs but Is Dispensable for endoHT and Hematopoiesis in the Yolk Sac

Whole-mount immunostaining of E9.5 yolk sacs localized KIT to small clusters of cells within the CDH5⁺ KDR⁺ endothelium that appeared rounder and smaller than neighboring ECs, consistent with imminent budding into the vascular lumen (Figures 1A,B). These observations support the idea that KIT is expressed by EMPs generated by hemogenic ECs undergoing endoHT and corroborate that KIT immunostaining distinguishes hemogenic from non-blood-forming ECs. We further found that CDH5 was

concentrated at adherens junctions at cell–cell contacts between KIT[−] ECs, consistent with its key role in joining ECs into vascular channels (Giannotta et al., 2013). Notably, KIT⁺ EMPs budding from the hemogenic endothelium had more intracellular CDH5 staining than neighboring ECs (Figures 1B,C, full arrowhead), and EMPs already released into the vessel lumen appeared negative for CDH5 by immunostaining (Figure 1C, empty arrowhead). These findings suggest that CDH5 internalization precedes EMP budding, presumably as a prerequisite for EMPs to break contact with the endothelial monolayer.

To identify EMPs with flow cytometry, KIT surface expression together with low levels of CD45 staining (CD45^{low}) has previously been combined with *Csf1r-iCre*-mediated lineage tracing (Gomez Perdiguero et al., 2015; Hoeffel et al., 2015) or with CD41 co-expression (McGrath et al., 2015; Frame et al., 2016). Using *Csf1r-iCre*-mediated lineage tracing with the recombination reporter *Rosa^{Yfp}* or *Rosa^{tdTom}*, we found that more than 80% of CD45^{low} YFP⁺ or TdTomato⁺ cells were also KIT⁺ in E9.5 yolk sacs (Figure 1D). Analysis of KIT surface expression with both CD41 and CD45 identified a KIT[−] cell population composed of CD45⁺ CD41[−] cells (Figure 1E) that likely correspond to myeloid cells (MCs) (McGrath et al., 2015; Frame et al., 2016) and CD45[−] CD41⁺ cells (Figure 1E) that likely correspond to megakaryoblasts (McGrath et al., 2015; Frame et al., 2016; Cortegano et al., 2019). By contrast, the KIT⁺ population (Figure 1E) included CD41^{low} cells, which were mostly CD45⁺. This cell population likely contains progenitors with definitive erythroid, myeloid, and lymphoid potential, including the previously described *Csf1r*-lineage traced CD45^{low} KIT⁺ EMPs (Gomez Perdiguero et al., 2015; Hoeffel et al., 2015) and CD45⁺ CD41⁺ KIT⁺ EMPs (McGrath et al., 2015; Frame et al., 2016), as well as lymphomyeloid progenitors (Boiers et al., 2013). The smaller proportion of KIT⁺ CD41^{low} progenitors that did not express CD45 (Figure 1E) may include EMPs that are CD45[−] (McGrath et al., 2015), possibly because they are less mature, as well as other KIT⁺ CD41⁺ CD45[−] hematopoietic precursors that have recently been described (Yamane, 2018).

To understand whether KIT promotes EMP formation and/or affects the differentiation potential of EMPs, we performed flow cytometry analysis of yolk sacs from mice lacking KIT. For this experiment, we used mice homozygous for the *Kit^{CreERT2}* knock-in allele, in which the *Cre* recombinase gene is inserted into the endogenous *Kit* locus (Klein et al., 2013) to generate a true *Kit* null allele (Heger et al., 2014). These mice are hereafter referred to as *Kit^{−/−}* mutants. Notably, KIT loss in E9.5 yolk sacs (Figure 2A) did not significantly alter the proportion or the number of the CD45[−] CD41[−] TER119⁺ erythroblasts (Frame et al., 2016), the CD45[−] CD41⁺ population that includes megakaryoblasts, the CD41^{low} progenitor population that includes both CD45⁺ and CD45[−] EMPs, or the CD45⁺ CD41[−] population corresponding to differentiating MCs (Figures 2B,C). Moreover, functional CFU-C assays with E9.5 yolk sac cells identified progenitors with either mixed erythro-myeloid (GEMMk: granulocyte, erythroid, monocyte/macrophage, megakaryocyte) or a more myeloid committed potential (GM: granulocyte, monocyte/macrophage; GMo: granulocyte, monocyte) in similar proportions in



KIT-deficient and littermate control embryos (**Figure 2D** and **Supplementary Figure 1**). By contrast, the number of functional progenitors in the mutants appeared reduced, albeit not at statistically significant levels (**Figure 2D**). Moreover, the colonies that grew from the mutant progenitors contained significantly fewer cells than those of wild-type littermates (**Figure 2D**), which indicates that the progenitors have reduced proliferative capacity.

Taken together, the analysis of KIT-deficient mice at E9.5 suggests that KIT is dispensable for primitive yolk sac hematopoiesis and for EMP formation from hemogenic

endothelium in the yolk sac, but that it is required cell autonomously in EMPs for their expansion.

KIT Is Dispensable for Yolk Sac-Derived Macrophage Colonization of Embryonic Organs

Yolk sac-born macrophages give rise to microglia (Schulz et al., 2012; Kierdorf et al., 2013; Gomez Perdiguero et al., 2015; Hoeffel et al., 2015). They also contribute to the initial pool of tissue-resident macrophages in several other developing organs,

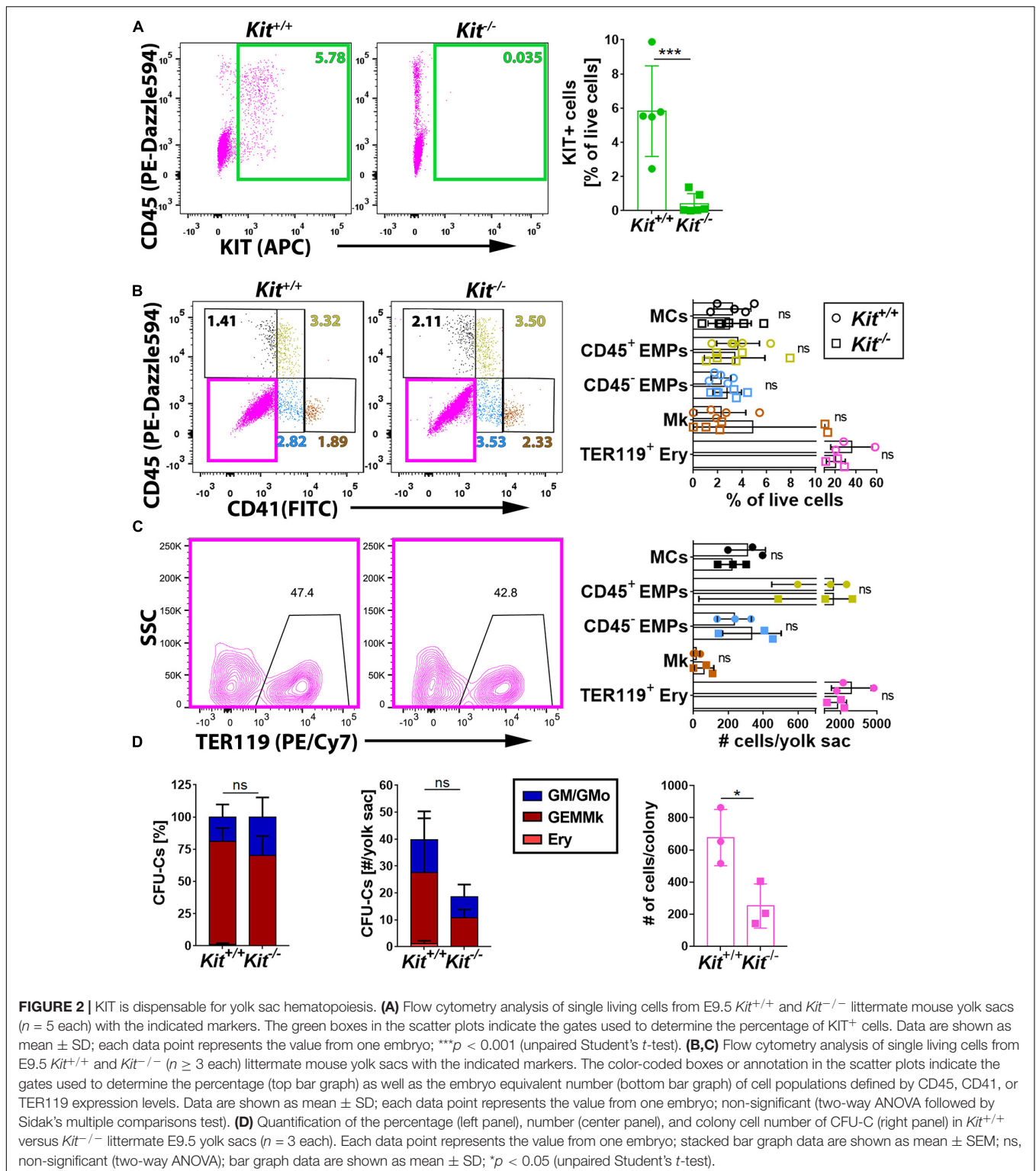
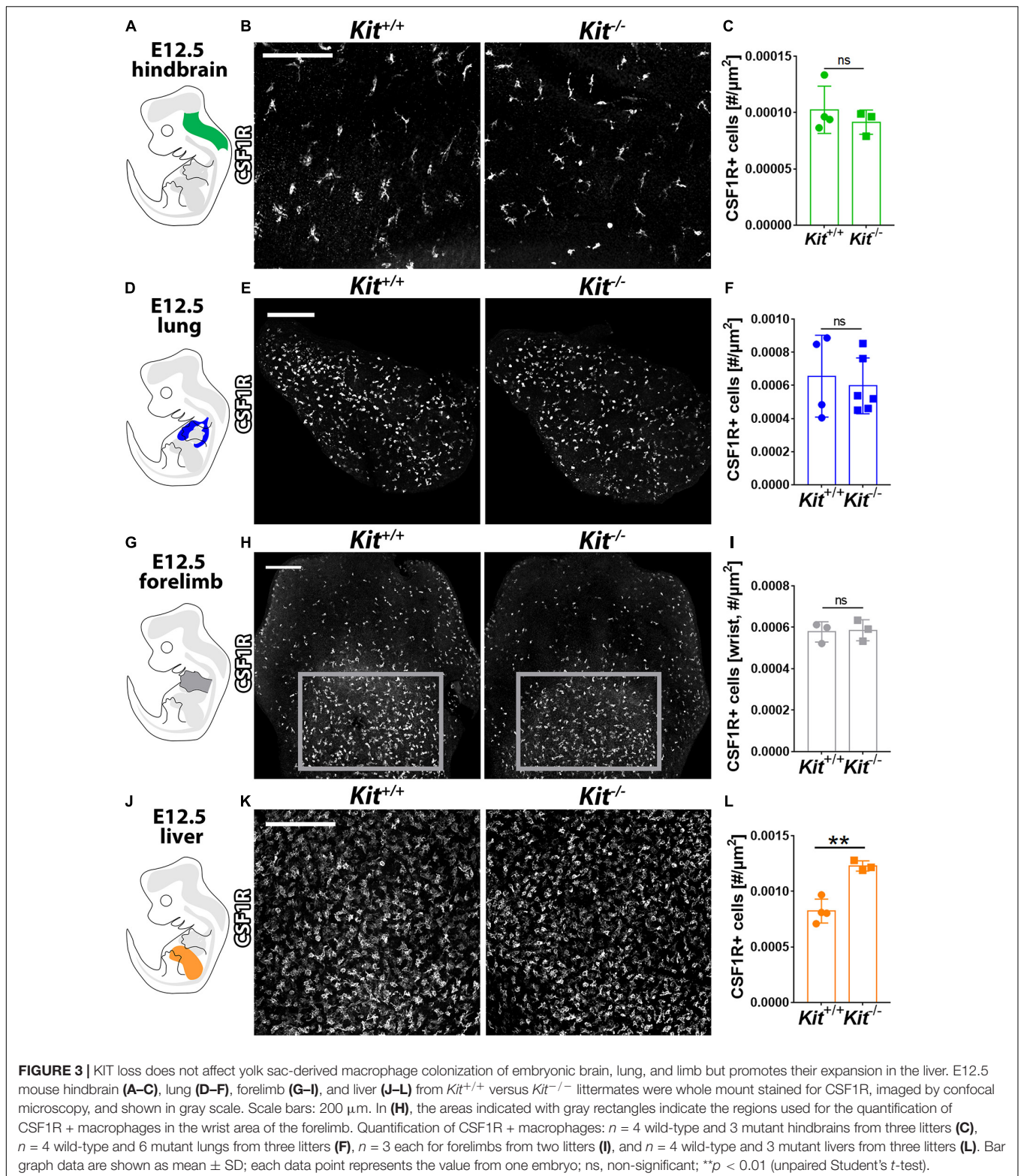


FIGURE 2 | KIT is dispensable for yolk sac hematopoiesis. **(A)** Flow cytometry analysis of single living cells from E9.5 *Kit*^{+/+} and *Kit*^{-/-} littermate mouse yolk sacs (*n* = 5 each) with the indicated markers. The green boxes in the scatter plots indicate the gates used to determine the percentage of KIT⁺ cells. Data are shown as mean ± SD; each data point represents the value from one embryo; ****p* < 0.001 (unpaired Student's *t*-test). **(B,C)** Flow cytometry analysis of single living cells from E9.5 *Kit*^{+/+} and *Kit*^{-/-} (*n* ≥ 3 each) littermate mouse yolk sacs with the indicated markers. The color-coded boxes or annotation in the scatter plots indicate the gates used to determine the percentage (top bar graph) as well as the embryo equivalent number (bottom bar graph) of cell populations defined by CD45, CD41, or TER119 expression levels. Data are shown as mean ± SD; each data point represents the value from one embryo; non-significant (two-way ANOVA followed by Sidak's multiple comparisons test). **(D)** Quantification of the percentage (left panel), number (center panel), and colony cell number of CFU-C (right panel) in *Kit*^{+/+} versus *Kit*^{-/-} littermate E9.5 yolk sacs (*n* = 3 each). Each data point represents the value from one embryo; stacked bar graph data are shown as mean ± SEM; ns, non-significant (two-way ANOVA); bar graph data are shown as mean ± SD; **p* < 0.05 (unpaired Student's *t*-test).

including lung, liver, and skin, where they constitute the main macrophage population at E12.5 (Hoeffel et al., 2015) before being complemented by monocytes derived from liver EMPs (Ginhoux and Guillemins, 2016). These yolk sac-derived tissue macrophages can be distinguished by high F4/80 and CSF1R

expression from the monocyte-derived macrophages derived from liver EMPs, which have low F4/80 levels (Schulz et al., 2012; Hoeffel et al., 2015). CSF1R immunofluorescence analysis showed that the number of microglia was similar between *Kit*^{+/+} and *Kit*^{-/-} hindbrains at E12.5 (Figures 3A–C). Moreover,



CSF1R immunostaining showed a similar number of tissue macrophages in the E12.5 lung and forelimb of *Kit*-null embryos and their wild-type littermates (Figures 3D–I). By contrast, the number of tissue macrophages in the E12.5 liver (termed Kupffer

cells) appeared significantly increased in mutants compared to wild-type controls (Figures 3J–L). KIT is therefore not required for the formation of yolk sac-derived macrophages (Figure 2) or their colonization of embryonic organs (Figure 3).

KIT Is Required for Transient-Definitive Fetal Liver Hematopoiesis

Starting from E10.5 onward, EMPs leave the yolk sac and colonize the fetal liver (Lux et al., 2008; Frame et al., 2013; Hoeffel et al., 2015; McGrath et al., 2015; Hoeffel and Ginhoux, 2018). To define the KIT⁺ cell populations in the fetal liver, we analyzed the E12.5 mouse liver transcriptome by scRNA-seq (detailed characterization in a manuscript in preparation). Consistent with the liver being the major hematopoietic organ at E12.5, our annotation identified several hematopoietic cell types in a UMAP continuum. Thus, a cluster of hematopoietic stem and progenitor cells (HSPCs, *Myb*⁺), composed mostly of EMPs and also the first HSCs, branched into several cell trajectories defined by markers of granulocytes (G, *Ly6g*⁺), monocytes and Kupffer cells (Mo/KC, *Fcgr1*⁺), megakaryocytes (Mk, *Pf4*⁺), or erythroid-committed progenitors such as burst-forming unit erythroid (BFU-E) cells (Ery, *Klf1*⁺ *Rhd*⁻) and erythroblasts (Eryb, *Klf1*⁺ *Rhd*⁺) (Figures 4A,B). As expected, we also identified distinct clusters of yolk sac-derived primitive orthochromatic erythroblasts (EryP, *Hba-x*⁺) as well as hepatoblasts (Hepa, *Alb*⁺) and ECs (*Cldn5*⁺) (Figure 4B).

We next examined which liver cell types expressed *Kit*. Hepatoblasts and fetal liver ECs did not contain *Kit* transcripts or the hemogenic endothelium marker *Runx1* (Figures 4C,D). These findings support the idea that the fetal liver, even though it harbors recruited hematopoietic progenitors (Lux et al., 2008; Frame et al., 2013; Hoeffel et al., 2015; McGrath et al., 2015; Hoeffel and Ginhoux, 2018), lacks hemogenic endothelium. *Kit* transcripts were also not detected in primitive erythroblasts, differentiating megakaryocytes, or differentiated MCs (Figures 4C,D). By contrast, *Kit* transcripts were abundant in the HSPC population that includes EMPs (Figures 4C,D). *Kit* transcripts were also abundant in erythroid-committed progenitors (BFU-E), but the number of *Kit*⁺ cells gradually decreased in erythroid-committed progenitors as they differentiated toward an erythroblast phenotype, with barely any *Kit*⁺ cells present in the erythroblast cluster (Figures 4C,D).

Liver EMPs can also be identified by flow cytometry in the E12.5 *Csf1r-iCre;Rosa^{tdTomato}* liver as CD45⁺ tdTomato⁺ cells lacking the differentiated MC marker CD11b. In agreement with the scRNA-seq data, we found that ~90% of EMPs in wild-type liver were KIT⁺ (Figure 4E). In contrast, CD45⁺ tdTomato⁺ CD11b⁺ cells mostly lacked KIT (Figure 4E), agreeing with the finding that *Kit* transcripts were not identified in differentiated MCs (Figures 4C,D). Moreover, KIT⁺ cells were also detected in the CD45⁻ population, both within the TER119⁺ erythroid cells and the TER119⁻ cells that likely include erythroid progenitors (Supplementary Figure 2). Immunostaining confirmed that KIT is expressed in large and round TER119⁻ cells that likely represent hematopoietic progenitors and only a few of the smaller TER119⁺ erythroblasts (Figure 4F), most likely proerythroblasts (Azzoni et al., 2018). This expression pattern is compatible with a selective role for KIT in hematopoietic progenitor populations that include EMPs and their erythroid-committed progeny during fetal liver erythropoiesis.

We next examined how KIT loss affected hematopoietic cells including EMP progeny in the liver (Figures 4G-I).

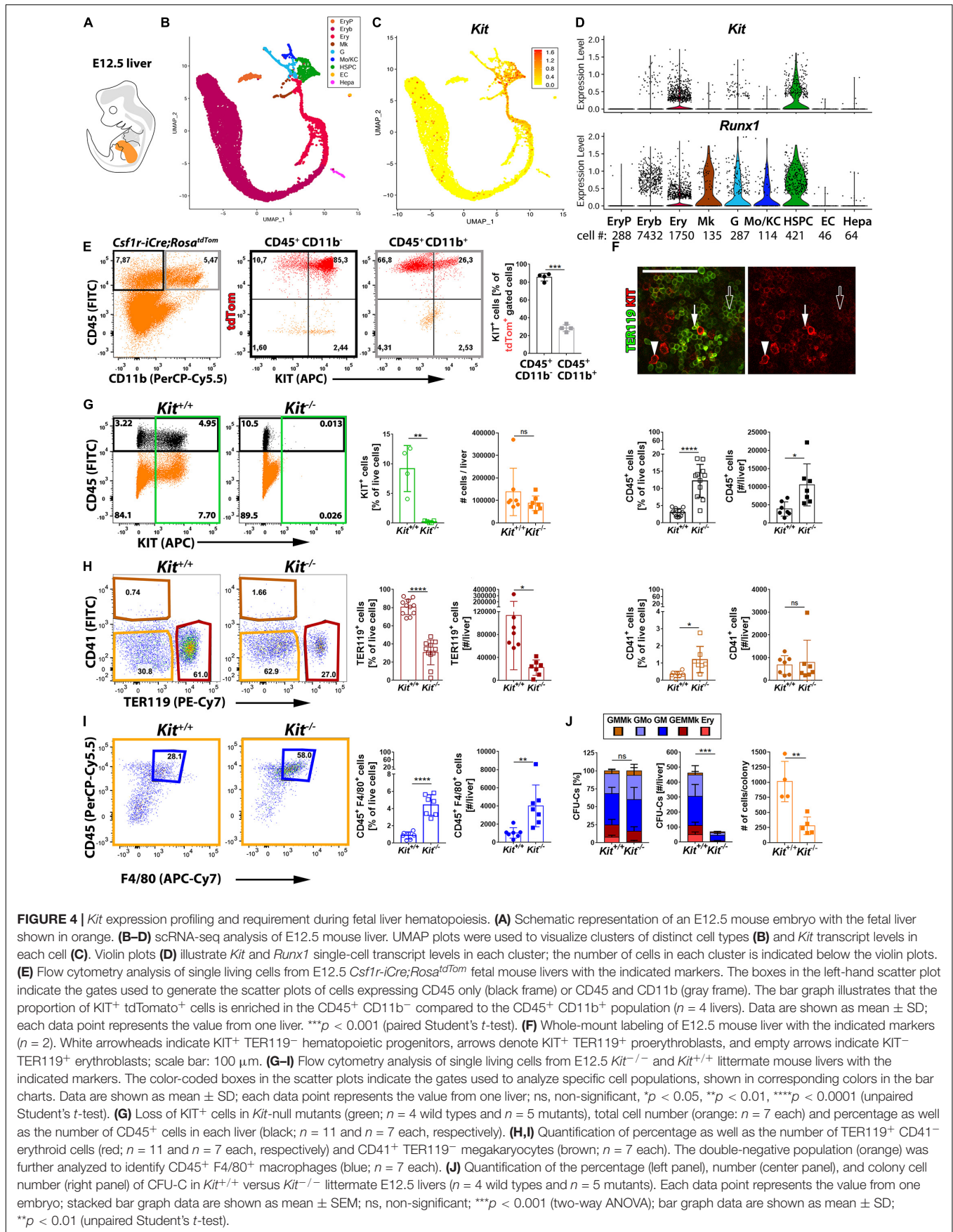
Overall, organ cellularity was similar in the liver of E12.5 KIT-deficient and wild-type mice (Figure 4G). Nevertheless, both the proportion and total number of TER119⁺ cells were significantly decreased in mutants (Figure 4H). By contrast, both the proportion and total number of CD45⁺ cells were significantly increased (Figure 4G). Additionally, the proportion of CD41⁺ megakaryocytes (Figure 4H) and both the proportion and total number of CD45⁺ F4/80⁺ macrophages (Figure 4I) were significantly increased. The increase in non-erythroid hematopoietic cells may explain why organ cellularity was not decreased in KIT-deficient livers, despite impaired erythropoiesis.

To better understand the origin of this hematopoietic imbalance, we compared the clonogenic potential of hematopoietic progenitors in the E12.5 liver from KIT-deficient and littermate control embryos. In both genotypes, we observed similar proportions of mixed erythro-myeloid progenitors (GEMMk) and progenitors with a more lineage-committed potential (GM; GMo; GMMk: granulocyte, monocyte/macrophage, megakaryocyte; Ery: erythroid) (Figure 4J and Supplementary Figure 1). Finding that the clonogenic potential of liver EMPs is preserved despite KIT deficiency implies that KIT does not play a role in fate decisions made by EMPs as they differentiate into committed progenitors in the fetal liver. Nevertheless, CFU-C assays revealed a significant decrease in the absolute number of clonogenic progenitors across all lineages in *Kit*-null livers, with virtually no erythroid or mixed erythro-myeloid colonies (Figure 4J). Moreover, the colonies produced by the remaining progenitors from mutant livers contained significantly fewer cells (Figure 4J). These results identify an essential role for KIT in progenitor expansion after their recruitment into the liver.

DISCUSSION

In recent years, it has become clear that EMPs form in the yolk sac but, starting from E10.5, they migrate from the yolk sac into the fetal liver (Palis and Yoder, 2001), where they expand and differentiate (Ginhoux and Williams, 2016). Our analysis showed KIT localization to a cluster of hematopoietic progenitors that appeared to bud from yolk sac ECs at E9.5 and therefore likely represent EMPs (Figure 1). Contrary to prior *ex vivo* findings, which concluded that KIT is required for hemogenic endothelial cell (EC) specification and function *ex vivo* (Marcelo et al., 2013), our flow cytometry analysis of KIT null mutants showed that KIT is dispensable for the generation of CD41^{low} progenitors, which include both CD45⁺ and CD45⁻ KIT⁺ EMPs (Figure 2). Furthermore, we found that KIT is dispensable for the formation of differentiated hematopoietic cells in the E9.5 yolk sac (Figure 2), which are generated by both primitive progenitors and the earliest wave of EMPs (Hoeffel and Ginhoux, 2018). These findings, in turn, suggest that hemogenic endothelium can form and function even in the absence of KIT to generate EMPs.

EMPs arising in E8.5 and E9.5 yolk sacs exhibit erythroid and broad myeloid, but not lymphoid potential (Frame et al., 2013; Ginhoux and Williams, 2016). Notably, we observed a diminished proliferative capacity for E9.5 yolk sac EMPs in



KIT-deficient mice, together with a trend for fewer clonogenic progenitors overall (**Figure 2**). This impairment became statistically significant in fetal liver of the E12.5 KIT-deficient mice, which showed a major decrease in the number of functional hematopoietic progenitors as well as their proliferative capacity (**Figure 4**). Our observations agree with a recent study of mice lacking the KIT ligand KITL (also known as stem cell factor, SCF), which is expressed by yolk sac and fetal liver ECs as well as fetal liver stromal cells (Azzoni et al., 2018). Specifically, this prior study reported the normal emergence of EMPs in the yolk sac at E9.5 but a striking decrease in their number in the fetal liver (Azzoni et al., 2018). This reduction in liver EMPs was ascribed to reduced EMP proliferation in the yolk sac after E9.5, which resulted in a decreased number of circulating EMPs and reduced their colonization, proliferation, and survival in the liver (Azzoni et al., 2018).

Our single-cell transcriptomic analysis of E12.5 fetal liver demonstrated that KIT transcripts are not detectable in ECs at this stage (**Figure 4**). Lack or low levels of *Kit* expression in E12.5 liver ECs is unexpected, because *Kit* is abundantly expressed in adult hepatic sinusoidal ECs (Mansuroglu et al., 2009); see also Tabula Muris database¹ (Tabula Muris Consortium et al., 2018). Our findings therefore suggest that robust *Kit* expression in liver ECs is acquired later on during development, perhaps after the liver vasculature has specialized into the sinusoids that connect the portal triads to the central veins (Strauss et al., 2017). Instead, KIT transcripts were enriched in liver hematopoietic progenitors, including EMPs and erythroid progenitors such as the BFU-E (**Figure 4**). This expression pattern agrees with the finding that KIT is required for EMP expansion, which starts in the E9.5 yolk sac downstream of EMP formation from the yolk sac hemogenic endothelium (**Figure 2**) and continues in the E12.5 liver (**Figure 4**). Moreover, *Kit* expression in liver erythroid progenitors is consistent with a KIT requirement for EMP-dependent transient-definitive erythropoiesis taking place in the fetal liver (**Figure 4**), a process that is required to sustain embryonic life until birth (Soares-da-Silva et al., 2021). Our study therefore provides new insights into the precise requirement of KIT in specific progenitor populations for developmental erythropoiesis. Specifically, our study refines previous work based on *Kit*^{W/W} and *Kitl*^{Sl/Sl} spontaneous mutants (Russell et al., 1968; Chui and Russell, 1974; Chui et al., 1978) and neutralizing anti-KIT antibodies (Ogawa et al., 1993), which showed an erythroid differentiation block in the fetal liver after E13.5 without identifying the specific progenitor population involved. Accordingly, we have identified EMP expansion and erythroid differentiation from EMP-derived progenitors in the fetal liver as the first events in which KIT acts to prevent severe anemia.

We further show that KIT is dispensable for the generation of tissue-resident macrophages in the E12.5 brain, lung, and limb bud (**Figure 3**). This finding agrees with KIT being dispensable for the generation of MCs in the yolk sac (**Figure 2**), because tissue macrophages in early embryonic organs are known to differentiate from hematopoietic progenitors that arise in the yolk sac before the birth of the liver-colonizing EMPs (Ginhoux and

Guilliams, 2016; Hoeffel and Ginhoux, 2018). Our observations also agree with findings in mice lacking KITL (Azzoni et al., 2018), in which the proportion of yolk sac-derived tissue macrophages (F4/80^{hi} CD11b^{lo}) in the brain, lungs, and limb buds are unaffected at E14.5 (Azzoni et al., 2018). However, we have also observed a notable difference between the analyses of KIT- and KITL-deficient mice. Thus, KIT-deficient mice have an increased population of yolk sac-derived macrophages in the E12.5 liver compared to wild-type littermates (**Figure 3**), but the liver of E11.5 or E14.5 KITL-deficient mice does not (Azzoni et al., 2018). It is not known whether this difference in ligand and receptor mutant mice is due to the different embryonic stages examined (E12.5 vs. 11.5 and E14.5) or whether defective liver hematopoiesis caused by KIT deficiency indirectly allows for early tissue macrophage expansion, whereas KITL deficiency does not.

Notably, the population of F4/80^{lo} CD11b^{hi} monocyte-derived macrophages, which are derived from fetal liver EMPs, is significantly reduced in the E14.5 liver lacking KITL (Azzoni et al., 2018). This observation is consistent with the reduced number of clonogenic fetal liver progenitors across all lineages and their reduced expansion, a phenotype that is observed for both E11.5 KITL-deficient mice (Azzoni et al., 2018) and E12.5 *Kit*-null mice (**Figure 4**). While we have not specifically examined whether the population of E14.5 monocyte-derived macrophages is affected downstream of the E12.5 EMP defect in *Kit*-null mice, it stands to reason that the overall increase in macrophage numbers in the liver of *Kit* mutants at E12.5 might be explained by a KIT deficiency-induced mechanism that promotes the self-renewal of yolk sac-derived macrophages to compensate for the reduction in liver EMP and EMP-derived cells, which are mostly erythroblasts at this stage.

The central finding of our study is the KIT requirement downstream of EMP formation in the yolk sac, with a key role in EMP expansion and regulating transient-definitive fetal liver hematopoiesis across several cell lineages to affect erythroid, myeloid, and megakaryocyte generation (see working model, **Supplementary Figure 3**). At E12.5, KIT loss has a major impact on fetal liver erythropoiesis, which normally peaks at E12.5 (McGrath et al., 2011; Iturri et al., 2021). By contrast, the reduction in myeloid output from liver EMPs in the mutants cannot yet be appreciated at E12.5, when the tissue macrophage population is still mostly of yolk sac origin (Hoeffel et al., 2015). Moreover, the local expansion of the yolk sac-derived macrophage population (**Figure 3**) would likely mask any deficiency in myeloid output from liver EMPs (**Supplementary Figure 3**, model). In agreement with our observation that KIT promotes erythroid development, gain-of-function mutations in the *Kit* coding sequence have been described to trigger clonal expansion of malignant pro-erythroblasts in murine erythroleukemia (Kosmider et al., 2005). Moreover, compatible with KIT regulating the expansion of EMPs with their intrinsic myeloid potential, gain-of-function mutations have been associated with human adult and pediatric core binding factor acute myeloid leukemia (CBF-AML), for which KIT mutations are poor prognostic factors (Cairoli et al., 2006; Krauth et al., 2014; Chen et al., 2018). It should therefore be

¹<https://tabula-muris.ds.czbiohub.org/>

investigated whether *KIT* mutations also contribute to human erythroleukemia.

METHODS

See **Supplementary Material**.

DATA AVAILABILITY STATEMENT

Fetal liver scRNAseq data can be found here: [https://www.ncbi.nlm.nih.gov/geo/, GSE180050]. The original contributions presented in the study are included in the article/**Supplementary Material**, further inquiries can be directed to the corresponding authors.

ETHICS STATEMENT

The animal study was reviewed and approved by the Animal Welfare Ethical Review Body (AWERB) and UK Home Office.

AUTHOR CONTRIBUTIONS

AF and CR contributed to the conception, design of the study, and co-wrote the manuscript. AF, CT, CR, and LD performed mouse experiments. AF and CT analyzed data. EV and EC performed bioinformatic analyses. All authors read and approved the submitted manuscript.

REFERENCES

- Azzoni, E., Frontera, V., McGrath, K. E., Harman, J., Carrelha, J., Nerlov, C., et al. (2018). Kit ligand has a critical role in mouse yolk sac and aorta-gonad-mesonephros hematopoiesis. *EMBO Rep.* 19:e45477.
- Bernex, F., De Sepulveda, P., Kress, C., Elbaz, C., Delouis, C., and Panthier, J. J. (1996). Spatial and temporal patterns of c-kit-expressing cells in WlacZ/+ and WlacZ/WlacZ mouse embryos. *Development* 122, 3023–3033. doi: 10.1242/dev.122.10.3023
- Boiers, C., Carrelha, J., Lutteropp, M., Luc, S., Green, J. C., Azzoni, E., et al. (2013). Lymphomyeloid contribution of an immune-restricted progenitor emerging prior to definitive hematopoietic stem cells. *Cell Stem Cell* 13, 535–548. doi: 10.1016/j.stem.2013.08.012
- Broudy, V. C. (1997). Stem cell factor and hematopoiesis. *Blood* 90, 1345–1364. doi: 10.1182/blood.v90.4.1345
- Cairolì, R., Beghini, A., Grillo, G., Nadali, G., Elice, F., Ripamonti, C. B., et al. (2006). Prognostic impact of c-KIT mutations in core binding factor leukemias: an Italian retrospective study. *Blood* 107, 3463–3468. doi: 10.1182/blood-2005-09-3640
- Canu, G., and Ruhrberg, C. (2021). First blood: the endothelial origins of hematopoietic progenitors. *Angiogenesis* 24, 199–211. doi: 10.1007/s10456-021-09783-9
- Chen, X., Dou, H., Wang, X., Huang, Y., Lu, L., Bin, J., et al. (2018). KIT mutations correlate with adverse survival in children with core-binding factor acute myeloid leukemia. *Leuk. Lymphoma* 59, 829–836. doi: 10.1080/10428194.2017.1361025
- Chui, D. H., and Loyer, B. V. (1975). Foetal erythropoiesis in steel mutant mice. II. Haemopoietic stem cells in foetal livers during development. *Br. J. Haematol.* 29, 553–565. doi: 10.1111/j.1365-2141.1975.tb02742.x

FUNDING

This study was supported by research grants from the Wellcome Trust to CR (095623/Z/11/Z), the British Heart Foundation to CR and AF (PG/18/85/34127), the Fondazione Cariplo to AF (2018-0298), and the Fondazione Associazione Italiana per la Ricerca sul Cancro (AIRC) to AF (22905). The funders had no role in the study design, data collection and interpretation, or the decision to submit the work for publication.

ACKNOWLEDGMENTS

We thank the staff of the Biological Resources, FACS and Imaging Facilities at the UCL Institute of Ophthalmology, the Genomics facility at European Institute of Oncology (IEO), the Unitech NOLIMITS Imaging facility at University of Milan, and Chiara Colletto for technical help. We thank Giulio Pavesi and Federico Zambelli for server access and Alison Domingues for helpful comments on the manuscript.

SUPPLEMENTARY MATERIAL

The Supplementary Material for this article can be found online at: <https://www.frontiersin.org/articles/10.3389/fcell.2021.648630/full#supplementary-material>

- Chui, D. H., and Russell, E. S. (1974). Fetal erythropoiesis in steel mutant mice. I. A morphological study of erythroid cell development in fetal liver. *Dev. Biol.* 40, 256–269. doi: 10.1016/0012-1606(74)90128-6
- Chui, D. H., Liao, S. K., and Walker, K. (1978). Fetal erythropoiesis in steel mutant mice. III. Defect in differentiation from BFU-E to CFU-E during early development. *Blood* 51, 539–547. doi: 10.1182/blood.v51.3.539.539
- Cortegano, I., Serrano, N., Ruiz, C., Rodriguez, M., Prado, C., Alia, M., et al. (2019). CD45 expression discriminates waves of embryonic megakaryocytes in the mouse. *Haematologica* 104, 1853–1865. doi: 10.3324/haematol.2018.192559
- Dejana, E., Hirschi, K. K., and Simons, M. (2017). The molecular basis of endothelial cell plasticity. *Nat. Commun.* 8:14361.
- Ding, L., Saunders, T. L., Enikolopov, G., and Morrison, S. J. (2012). Endothelial and perivascular cells maintain haematopoietic stem cells. *Nature* 481, 457–462.
- Fleischman, R. A., and Mintz, B. (1979). Prevention of genetic anemias in mice by microinjection of normal hematopoietic stem cells into the fetal placenta. *Proc. Natl. Acad. Sci. U.S.A.* 76, 5736–5740. doi: 10.1073/pnas.76.11.5736
- Frame, J. M., Fegan, K. H., Conway, S. J., McGrath, K. E., and Palis, J. (2016). Definitive hematopoiesis in the yolk sac emerges from wnt-responsive hemogenic endothelium independently of circulation and arterial identity. *Stem Cells* 34, 431–444. doi: 10.1002/stem.2213
- Frame, J. M., McGrath, K. E., and Palis, J. (2013). Erythro-myeloid progenitors: “definitive” hematopoiesis in the conceptus prior to the emergence of hematopoietic stem cells. *Blood Cells Mol. Dis.* 51, 220–225. doi: 10.1016/j.bcmd.2013.09.006
- Giannotta, M., Trani, M., and Dejana, E. (2013). VE-cadherin and endothelial adherens junctions: active guardians of vascular integrity. *Dev. Cell* 26, 441–454. doi: 10.1016/j.devcel.2013.08.020
- Ginhoux, F., and Williams, M. (2016). Tissue-resident macrophage ontogeny and homeostasis. *Immunity* 44, 439–449. doi: 10.1016/j.immuni.2016.02.024

- Goldie, L. C., Lucitti, J. L., Dickinson, M. E., and Hirschi, K. K. (2008). Cell signaling directing the formation and function of hemogenic endothelium during murine embryogenesis. *Blood* 112, 3194–3204. doi: 10.1182/blood-2008-02-139055
- Gomez Perdiguero, E., Klapproth, K., Schulz, C., Busch, K., Azzoni, E., Crozet, L., et al. (2015). Tissue-resident macrophages originate from yolk-sac-derived erythro-myeloid progenitors. *Nature* 518, 547–551. doi: 10.1038/nature13989
- Hashimoto, D., Chow, A., Noizat, C., Teo, P., Beasley, M. B., Leboeuf, M., et al. (2013). Tissue-resident macrophages self-maintain locally throughout adult life with minimal contribution from circulating monocytes. *Immunity* 38, 792–804. doi: 10.1016/j.immuni.2013.04.004
- Heger, K., Seidler, B., Vahl, J. C., Schwartz, C., Kober, M., Klein, S., et al. (2014). CreER(T2) expression from within the c-Kit gene locus allows efficient inducible gene targeting in and ablation of mast cells. *Eur. J. Immunol.* 44, 296–306. doi: 10.1002/eji.201343731
- Hoefel, G., and Ginhoux, F. (2018). Fetal monocytes and the origins of tissue-resident macrophages. *Cell. Immunol.* 330, 5–15. doi: 10.1016/j.cellimm.2018.01.001
- Hoefel, G., Chen, J., Lavin, Y., Low, D., Almeida, F. F., See, P., et al. (2015). C-Myb(+) erythro-myeloid progenitor-derived fetal monocytes give rise to adult tissue-resident macrophages. *Immunity* 42, 665–678. doi: 10.1016/j.immuni.2015.03.011
- Ikuta, K., and Weissman, I. L. (1992). Evidence that hematopoietic stem cells express mouse c-kit but do not depend on steel factor for their generation. *Proc. Natl. Acad. Sci. U.S.A.* 89, 1502–1506. doi: 10.1073/pnas.89.4.1502
- Iturri, L., Freyer, L., Biton, A., Dardenne, P., Lallemand, Y., and Gomez Perdiguero, E. (2021). Two Sequential and Independent Pathways of Erythromyeloid Progenitor Commitment in Their Niche of Emergence. Available online at: <https://ssrn.com/abstract=3732381>
- Kierdorf, K., Erny, D., Goldmann, T., Sander, V., Schulz, C., Perdiguero, E. G., et al. (2013). Microglia emerge from erythromyeloid precursors via Pu.1- and Irf8-dependent pathways. *Nat. Neurosci.* 16, 273–280. doi: 10.1038/nn.3318
- Klein, S., Seidler, B., Kettenberger, A., Sibaev, A., Rohn, M., Feil, R., et al. (2013). Interstitial cells of Cajal integrate excitatory and inhibitory neurotransmission with intestinal slow-wave activity. *Nat. Commun.* 4:1630.
- Kosmider, O., Denis, N., Lacout, C., Vainchenker, W., Dubreuil, P., and Moreau-Gachelin, F. (2005). Kit-activating mutations cooperate with Spi-1/PU.1 overexpression to promote tumorigenic progression during erythroleukemia in mice. *Cancer Cell* 8, 467–478. doi: 10.1016/j.ccr.2005.11.009
- Krauth, M. T., Eder, C., Alpermann, T., Bacher, U., Nadarajah, N., Kern, W., et al. (2014). High number of additional genetic lesions in acute myeloid leukemia with t(8; 21)/RUNX1-RUNX1T1: frequency and impact on clinical outcome. *Leukemia* 28, 1449–1458. doi: 10.1038/leu.2014.4
- Lux, C. T., Yoshimoto, M., McGrath, K., Conway, S. J., Palis, J., and Yoder, M. C. (2008). All primitive and definitive hematopoietic progenitor cells emerging before E10 in the mouse embryo are products of the yolk sac. *Blood* 111, 3435–3438. doi: 10.1182/blood-2007-08-107086
- Mansuroglu, T., Ramadori, P., Dudas, J., Malik, I., Hammerich, K., Fuzesi, L., et al. (2009). Expression of stem cell factor and its receptor c-Kit during the development of intrahepatic cholangiocarcinoma. *Lab. Invest.* 89, 562–574. doi: 10.1038/labinvest.2009.15
- Marcelo, K. L., Sills, T. M., Coskun, S., Vasavada, H., Sanglikar, S., Goldie, L. C., et al. (2013). Hemogenic endothelial cell specification requires c-Kit, Notch signaling, and p27-mediated cell-cycle control. *Dev. Cell* 27, 504–515. doi: 10.1016/j.devcel.2013.11.004
- McGrath, K. E., Frame, J. M., Fegan, K. H., Bowen, J. R., Conway, S. J., Catherman, S. C., et al. (2015). Distinct sources of hematopoietic progenitors emerge before HSCs and provide functional blood cells in the mammalian embryo. *Cell Rep.* 11, 1892–1904. doi: 10.1016/j.celrep.2015.05.036
- McGrath, K. E., Frame, J. M., Fromm, G. J., Koniski, A. D., Kingsley, P. D., Little, J., et al. (2011). A transient definitive erythroid lineage with unique regulation of the beta-globin locus in the mammalian embryo. *Blood* 117, 4600–4608. doi: 10.1182/blood-2010-12-325357
- Ogawa, M., Nishikawa, S., Yoshinaga, K., Hayashi, S., Kunisada, T., Nakao, J., et al. (1993). Expression and function of c-Kit in fetal hemopoietic progenitor cells: transition from the early c-Kit-independent to the late c-Kit-dependent wave of hemopoiesis in the murine embryo. *Development* 117, 1089–1098. doi: 10.1242/dev.117.3.1089
- Palis, J., and Yoder, M. C. (2001). Yolk-sac hematopoiesis: the first blood cells of mouse and man. *Exp. Hematol.* 29, 927–936. doi: 10.1016/s0301-472x(01)00669-5
- Russel, E. S., Thompson, M. W., and McFarland, E. (1968). Analysis of effects of W and f genic substitutions on fetal mouse hematology. *Genetics* 58, 259–270. doi: 10.1093/genetics/58.2.259
- Rybtsov, S., Batsivari, A., Bilotkach, K., Paruzina, D., Senserrich, J., Nerushev, O., et al. (2014). Tracing the origin of the HSC hierarchy reveals an SCF-dependent, IL-3-independent CD43(-) embryonic precursor. *Stem Cell Rep.* 3, 489–501. doi: 10.1016/j.stemcr.2014.07.009
- Rybtsov, S., Sobiesiak, M., Taoudi, S., Souilhol, C., Senserrich, J., Liakhovitskaia, A., et al. (2011). Hierarchical organization and early hematopoietic specification of the developing HSC lineage in the AGM region. *J. Exp. Med.* 208, 1305–1315. doi: 10.1084/jem.20102419
- Sanchez, M. J., Holmes, A., Miles, C., and Dzierzak, E. (1996). Characterization of the first definitive hematopoietic stem cells in the AGM and liver of the mouse embryo. *Immunity* 5, 513–525. doi: 10.1016/s1074-7613(00)80267-8
- Schulz, C., Gomez Perdiguero, E., Chorro, L., Szabo-Rogers, H., Cagnard, N., Kierdorf, K., et al. (2012). A lineage of myeloid cells independent of Myb and hematopoietic stem cells. *Science* 336, 86–90. doi: 10.1126/science.1219179
- Soares-da-Silva, F., Freyer, L., Elsaid, R., Burlen-Defranoux, O., Iturri, L., Sismeiro, O., et al. (2021). Yolk sac, but not hematopoietic stem cell-derived progenitors, sustain erythropoiesis throughout murine embryonic life. *J. Exp. Med.* 218:e20201729.
- Strauss, O., Phillips, A., Ruggiero, K., Bartlett, A., and Dunbar, P. R. (2017). Immunofluorescence identifies distinct subsets of endothelial cells in the human liver. *Sci. Rep.* 7:44356.
- Tabula Muris Consortium, Overall Coordination, Logistical Coordination, Organ Collection and Processing, Library Preparation and Sequencing, Computational Data Analysis, et al. (2018). Single-cell transcriptomics of 20 mouse organs creates a Tabula Muris. *Nature* 562, 367–372. doi: 10.1038/s41586-018-0590-4
- Taoudi, S., Gonneau, C., Moore, K., Sheridan, J. M., Blackburn, C. C., Taylor, E., et al. (2008). Extensive hematopoietic stem cell generation in the AGM region via maturation of VE-cadherin+CD45+ pre-definitive HSCs. *Cell Stem Cell* 3, 99–108. doi: 10.1016/j.stem.2008.06.004
- Waskow, C., Paul, S., Haller, C., Gassmann, M., and Rodewald, H. R. (2002). Viable c-Kit(W/W) mutants reveal pivotal role for c-kit in the maintenance of lymphopoiesis. *Immunity* 17, 277–288. doi: 10.1016/s1074-7613(02)00386-2
- Waskow, C., Terszowski, G., Costa, C., Gassmann, M., and Rodewald, H. R. (2004). Rescue of lethal c-KitW/W mice by erythropoietin. *Blood* 104, 1688–1695. doi: 10.1182/blood-2004-04-1247
- Yamane, T. (2018). Mouse yolk sac hematopoiesis. *Front. Cell Dev. Biol.* 6:80. doi: 10.3389/fcell.2018.00080
- Yokomizo, T., and Dzierzak, E. (2010). Three-dimensional cartography of hematopoietic clusters in the vasculature of whole mouse embryos. *Development* 137, 3651–3661. doi: 10.1242/dev.051094

Conflict of Interest: The authors declare that the research was conducted in the absence of any commercial or financial relationships that could be construed as a potential conflict of interest.

Publisher's Note: All claims expressed in this article are solely those of the authors and do not necessarily represent those of their affiliated organizations, or those of the publisher, the editors and the reviewers. Any product that may be evaluated in this article, or claim that may be made by its manufacturer, is not guaranteed or endorsed by the publisher.

Copyright © 2021 Fantin, Tacconi, Villa, Ceccacci, Denti and Ruhrberg. This is an open-access article distributed under the terms of the Creative Commons Attribution License (CC BY). The use, distribution or reproduction in other forums is permitted, provided the original author(s) and the copyright owner(s) are credited and that the original publication in this journal is cited, in accordance with accepted academic practice. No use, distribution or reproduction is permitted which does not comply with these terms.